20th International Conference on Renewable Energies and Power Quality (ICREPQ'22)
Vigo (Spain), 27th to 29th July 2022
Renewable Energy and Power Quality Journal (RE&PQJ)
ISSN 2172-038 X, Volume No.20, September 2022

Pin-hole free $MAPb_{0.75}Sn_{0.25}(I_{0.5}Br_{0.5})_3$ films spin casted without anti-solvent by adding MAAc additive to Perovskite ink

C. Q. Howlader[1], N. Khakurel[1], D.W. Amyx[3], W. Geerts[1,3], G. Gibson[4], and M. Chen[1,2]

[1] Department of Materials Science, Engineering, and Commercialization
[2]Ingram School of Engineering
[3]Department of Physics
Texas State University
San Marcos, Texas 78666 (USA)
Phone/Fax number: +1 512 210 7312, e-mail: cqh1@txstate.edu, yc12@txstate.edu

[4]FAS Holding Group
10480 Markison Road, Dallas, TX 75238, USA.
Phone/Fax number: +1 214 343 5304, e-mail: g.gibson@nTact.com

Abstract. To start the crystallization of the tin (Sn) based perovskite materials, anti-solvent treatment is a useful technique. But the use of anti-solvents increases the complexity of the deposition process thus hinders the applicability in mass production processes. Here we have developed an anti-solvent free $MAPb_{0.75}Sn_{0.25}(I_{0.50}Br_{0.50})_3$ perovskite thin film deposition method based on a one step spin coating process. Addition of 0 - 100 mol% of methylammonium acetate (MAAc) to the precursor ink allows for the deposition of continuous films. Films casted from ink with less than 60 mol% MAAc show pinholes and are rough. A decent crystalline and pin-hole free perovskite thin film can be obtained from 60 or more mol% MAAc additive. These results are confirmed by XRD, AFM and SEM measurements. $MAPb_{0.75}Sn_{0.25}(I_{0.50}Br_{0.50})_3$ has a wide bandgap and is currently being considered for applications in tandem solar cells and under water solar cells.

Key words. Perovskite, methylammonium acetate (MAAc), anti-solvent, crystallinity, grain-size.

1. Introduction

Hybrid perovskite materials show excellent photovoltaic properties and attracted worldwide attention for its power conversion efficiency in solar cells. Within a decade of research on the perovskite solar cells (PSC) its power conversion efficiency has reached more than 25% [1]. However, most efficient PSCs contain lead (Pb) and that is very unlikely to metabolize by organisms, thus has a great negative effect on the environment as well as human beings [2][3]. On the contrary, tin (Sn) could be an alternate for the Pb in the perovskite materials. However, tin-based PSCs might suffer from lower power conversion efficiency (PCE) and instability issues [4][5]. In the past years, researchers have become more interested in the Sn-Pb binary PSCs to reduce the environmental footprint the Pb based perovskite have. Y. Ogomi et al. fabricated the first Sn-Pb binary perovskite solar cells in 2014 with a PCE of 4.18% using an n-i-p device structure [6]. This perovskite is suitable to collect the solar energy in the near-infrared part of solar spectrum. However, electronic absorption for perovskite toward shorter wavelength region is also necessary for different applications such as tandem solar cells or solar cells for under water applications [7]. Till now, a tremendous amount of research is going on to improve the film quality, increase the bandgap as well as improve the PCE. The bandgap can be tuned easily by compositional engineering and inclusion of different halide anions in the perovskite structure. It is very common to achieve wide bandgap perovskite by simultaneous incorporation of Br and I halide anions. Tosado et al. increased the bandgap of Sn-Pb based perovskite to 1.30 eV by incorporating 17% of Br and obtained a PCE of 11.05 %, where they also utilized 75% of Sn as well [8]. The PCE of Sn-Pb based perovskite solar cells was further improved to 17.63% by reducing Sn content to 50% and increase the bandgap to 1.35 eV by adding 20% of Br [9]. Yang et al. made a perovskite with a bandgap of 1.73 eV by incorporating 60% of Br into Sn-Pb based perovskite and obtained a PCE of 12.59 % [7]. Within a short period of time, researchers were able to obtain more than 20% of PCE from Sn-Pb based PSCs [1][2][10]. However, most of them use anti-solvent to start the crystallization while depositing the perovskite precursor solution [7][8][9][11][12][13][14] As a result, such approach introduces complexity in the deposition process and hinders the application of mass production deposition processes such as slot-die and roll-to-roll deposition methods. Also, most of the anti-solvents are toxic in nature, another reason to avoid these [2].

In this work, we developed a process to deposit $MAPb_{0.75}Sn_{0.25}(I_{0.50}Br_{0.50})_3$ without anti-solvent by introducing Methyl ammonium acetate (MAAc) as additive in the $MAPb_{0.75}Sn_{0.25}(I_{0.50}Br_{0.50})_3$ precursor solution. The effects of MAAc in the perovskite ink on the physical properties of thin films casted by spin coating was

investigated by SEM. XRD, AFM, UV-Vis, and ellipsometry. A high-quality pin-hole free Sn-Pb based perovskite film can be obtained by increasing the amount of MAAc in the precursor solution to and above 60 mol%.

2. Experimental methods

A. Sample preparations

Commercially available chemicals purchased from Alpha Aesar and Sigma Aldrich were used to make the precursor solutions. To prepare Sn-Pb precursor solution, 50 mol% MAI, 50 mol% MABr, 37.5 mol% PbI_2, 37.5 mol% $PbBr_2$, 12.5 mol% SnI_2 and 12.5 mol% $SnBr_2$ were dissolved in one ml of DMF solvent and stirred at 500 rpm on a hot plate at 70° C for 1 hour. Different mol% (20, 40, 60, 80 and 100) of MAAc were added to the ink later on. All inks were filtered using a 0.22 μm PTFE filters before use. Glass microscope slides were cleaned ultrasonically in 5% Deconex in DI water followed by 20 minutes ultrasonically cleaning in DI water. Cleaned substrates were dried with nitrogen gas followed by additional cleaning in an air plasma (300 Watt) for 10 minutes.

The perovskite precursor solution was then deposited on the cleaned glass substates using a spin coater inside a N_2 glovebox. Spin coating was done at 4000 rpm for 60 sec without the use of antisolvent. Spun samples were annealed in a nitrogen atmosphere at 110°C for 15 min on a hotplate.

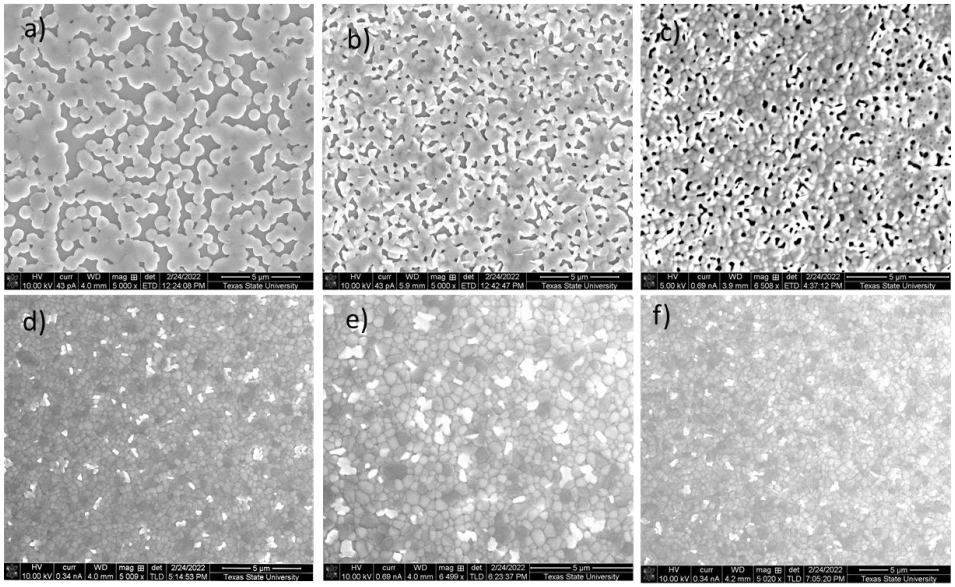

Fig.1. SEM image of MAPb0.75Sn0.25(I0.50Br0.50)3 with a) 0%, b) 20%, c) 40%, d) 60%, e) 80% and f)100% of MAAc

B. Sample characterizations

Thin films were characterized by different tools to determine the physical and optical properties. Θ-2θ XRD

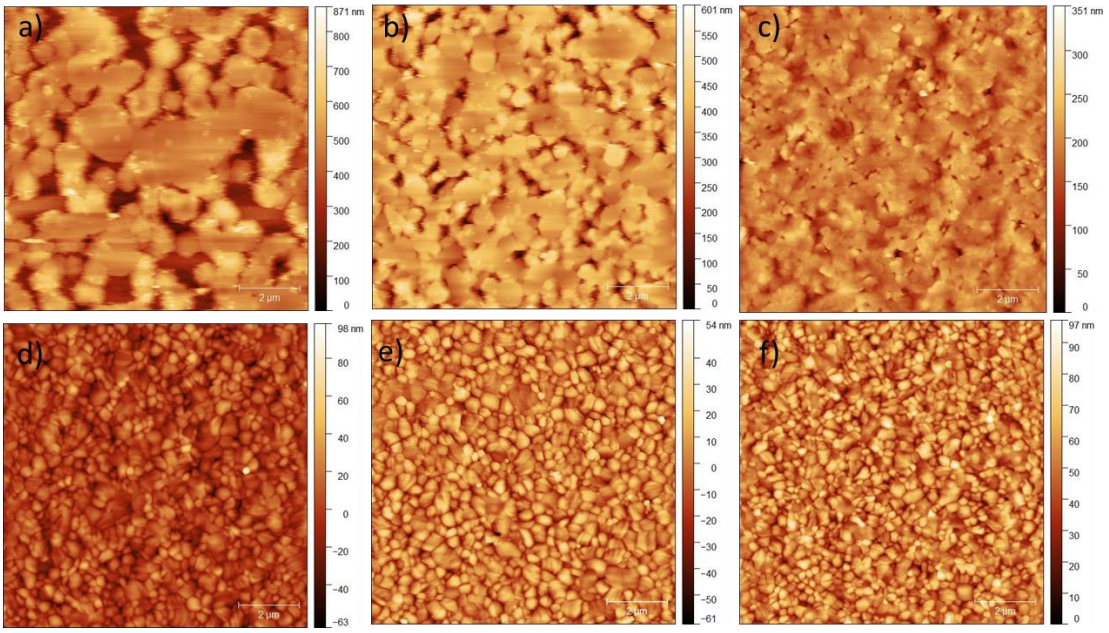

Fig.2. AFM image of MAPb0.75Sn0.25(I0.50Br0.50)3 with a) 0%, b) 20%, c) 40%, d) 60%, e) 80% and f)100% of MAAc

spectra were measured by a Rigaku SmartLab X-ray Diffractometer (XRD) with Cu target at 40 KeV. SEM pictures were taken by a FEI Helios NanoLab 400 DualBeam SEM with ETD. Topographic AFM pictures were taken by a Bruker Dimension ICON AFM using the HQ:NSC15/Al BS tip. Thicknesses were measured using a KLA Tencor P7 stylus profilometer. UV-Vis spectra were measured using a Shimadzu UV-2600 spectrometer to determine the absorption spectra. Optical properties such as refractive index and extinction coefficient were measured by a J.A. Woollam Co. M-2000UI ellipsometer for the wavelength range of 300 nm to 1600 nm.

AFM images are shown in Fig. 2. They also support the claim that coverage and roughness of the films depend significantly on the ink's MAAc concentration up to 60 mol% of MAAc. Films spun from an ink containing 0 and 100 mol% MAAc shows a roughness of around ~102 nm and ~12 nm, respectively. The roughnesses of all the films were determined by analysing the AFM images using the Gwyddion software and are shown in table 1. Note that changing the MAAc concentration from 60 to 100 mol% does not have a significant effect on film roughness. Also, there is a very little thickness variation of films spun using inks containing a MAAc concentration of 60 mol% or higher. They all have similar film thickness around ~237

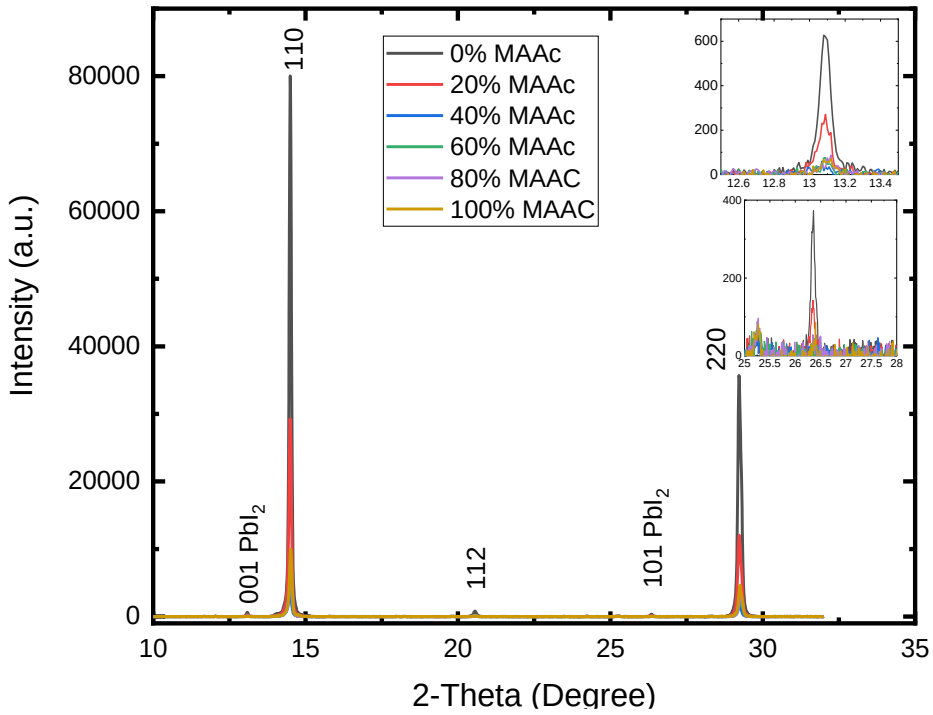

Fig.3. XRD spectra of $MAPb_{0.75}Sn_{0.25}(I_{0.50}Br_{0.50})_3$ contains different mol% of MAAc

3. Results and discussions

Incorporating MAAc in MAPI perovskite ink has shown to impact the nucleation and growth during deposition and result in a pin-hole free layer with good PCE [16]. The formation of perovskite is happening through exchange between X^- anion of MA^+X^- and Ac^- anion of an intermediate phase [15]. The MAAC does not stay in the film, but is evaporated out during the annealing step [16]. Here we explore if this same approach is also working for Sn-Pb based perovskites. Figure 1 shows the Scanning electron microscopy (SEM) images of films casted with ink containing different MAAc concentration. It is clear from the image that films casted from ink that does not contain MAAc contain a large number of pinholes and the number of pinholes is decreasing with the increase of MAAc in the precursor solution. To get a full coverage perovskite thin film we need to utilize more than 50 mol% of MAAc in the $MAPb_{0.75}Sn_{0.25}(I_{0.50}Br_{0.50})_3$ perovskite ink precursor solution. Note from Fig. 1 that the excess MAAc beyond 60 mol% does not have a reverse effect on the coverage of the perovskite film.

nm. The film thicknesses of all samples are summarized in the table 1.

The films were characterized by X-ray diffraction to determine the phase ID, grain size, and crystallinity. It has been reported that the most stable $MASnI_3$ phase at RT is the pseudo-cubic (P4mm) α-phase and the most stable RT MAPbI3 phase the tetragonal (I4mm) β-phase [12]. Figure 3 shows the measured Θ-2θ XRD spectra of perovskite films spun with ink with different MAAc molar concentrations. All of them show very strong perovskite characteristic peaks which match with the spectra reported in literature [5][9]. All observed peaks could be assigned to the α – phase. The films have a strong (110) and (220) texture for all MAAc concentrations. It is clearly identified that the (110) is the dominating plane for all cases. However, the (110) peak intensity decreases with increasing MAAc content in the precursor solution. This indicates a reduction of crystallinity of the thin films which was confirmed from the XRD spectra. The crystallinity of the films was determined from the Θ-2θ scans by dividing the surface

Table 1: Properties of $MAPb_{0.75}Sn_{0.25}(I_{0.50}Br_{0.50})_3$ thin film contains 0 mol% to 100 mol5 of MAAc

Sample type	Thickness (nm)	Roughness (nm)	Grain size (nm)	n@632.8 nm	Bandgap (eV)
0 mol%	362.24	102.4	76.19	--	1.62
20 mol%	261.74	62.37	69.46	--	1.60
40 mol%	296.16	28.08	62.38	--	1.63
60 mol%	231.84	14.34	64.53	2.38	1.63
80 mol%	237.19	12.77	69.25	2.34	1.63
100 mol%	237.16	13.61	64.05	2.40	1.63

area under the peaks by the surface area of the background signal using scans from 10 to 32 degrees. This analysis indicates a reduction of crystallinity for films spun with inks with increasing MAAc content. The grain size of the films determined from the XRD spectra using the Scherrer equation shows that grain size slightly decreases with the ink's MAAc concentration. From the XRD spectra, it's also detected that the films spun with ink with a low MAAc concentration have small PbI_2 and facilitates the crystal growth mostly at the 110 and 220 orientations.

For the solar cell's applications, it is also necessary to verify the optical properties along with other characterizations to know the photo response of the film. Figure 4 (left) shows the UV-Vis spectra of the Sn-Pb binary perovskite thin films for the range of 400 nm to 1100 nm. The absorption band edges start around 760 nm for films spun from inks of any MAAc concentration.

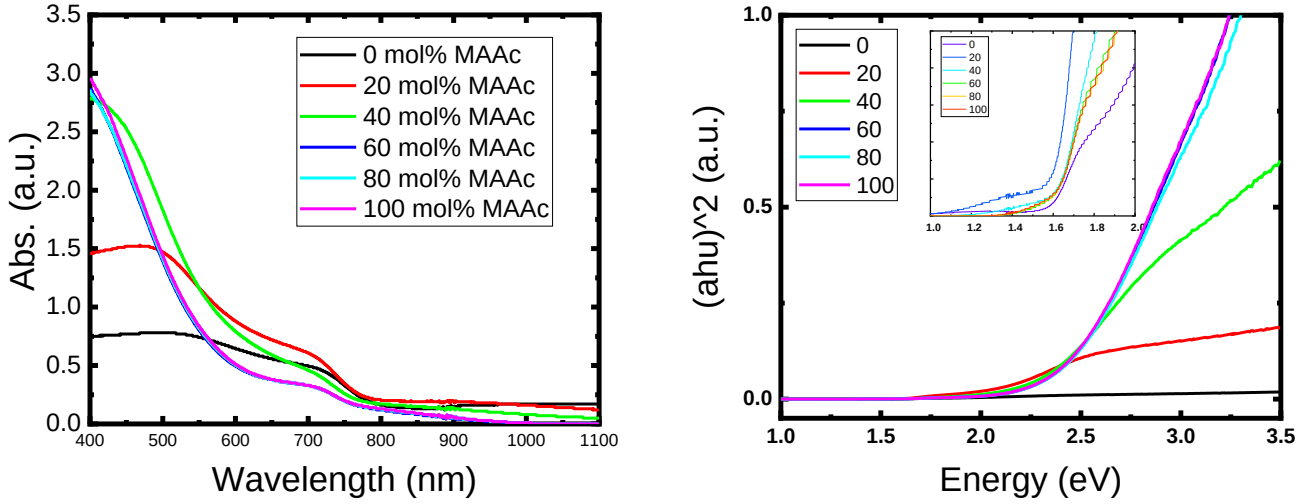

Fig 4: UV-Vis spectra (left) and Tauc plot (right) of $MAPb_{0.75}Sn_{0.25}(I_{0.50}Br_{0.50})_3$ contains different mol% of MAAc

peaks at 13.1 and 26.26 degrees which almost disappear for films spun from ink containing more than 60 mol% MAAc. The crystal size determined from the width of these PbI_2 peaks is 106.74 nm. It's clear from the spectra that the MAAc in the ink suppresses the lead iodide peaks

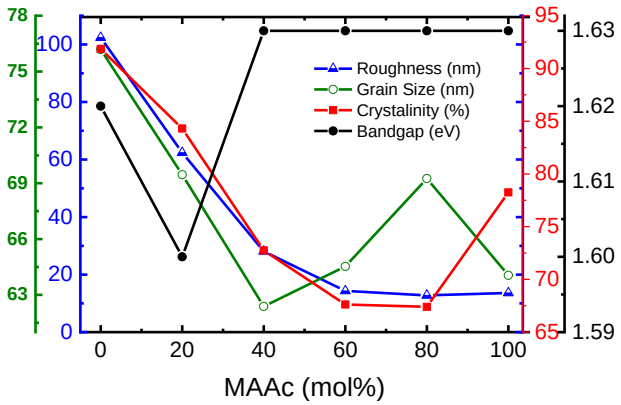

Fig. 5: Properties of $MAPb_{0.75}Sn_{0.25}(I_{0.50}Br_{0.50})_3$ Vs different mol% of MAAc

However, the pristine perovskite film shows different absorption behaviour around the shorter wavelength region. The absorption profile significantly changes for the shorter wavelength region while adding more MAAc in the perovskite precursor solution. It is speculated that this is due to (1) the low MAAc films were not continuous so UV light can transmit through the pinholes, (2) possibly an intermediate phase is formed in the perovskite thin films spin casted from high MAAc concentration inks [17]. The steep absorption edge observed around 760 nm confirms the formation of a continuous perovskite layer with a high absorption coefficient above 2.5 eV attributed of the black α-perovskite phase. To further study the effect of the ink's MAAc concentration on the bandgap of the Sn-Pb perovskite thin films, Tauc plots are drawn from the absorption spectra shown in figure 4 (right). Bandgaps of the films were obtained from the Tauc plot shown in the insert figure of figure 4 (right). The estimated bandgaps are presented in table 1 and are in agreement with the results reported by others for perovskite films with similar

composition [7]. These results confirm that the MAAc additive in the ink does not affect the optical properties of these films. Note that the absorption spectra of films spin casted from high MAAc concentration inks show a similar absorption profile suggesting that MAAc is not incorporated in the films. To further check the effect of excess MAAc in the precursor solution on the optical properties, we determined the refractive indices of the samples from spectroscopic ellipsometry measurements obtained with a Woollam M2000 ellipsometer. The ellipsometry data was fit with a B-spline model. The calculated optical spectra are consistent with the UV/VIS transmission spectrum [18][19]. After verifying the spectroscopic model, it is confirmed that the MAAc do not change the optical properties. The 632.8 nm refractive indices are summarized in table 1. Figure 5 shows the effect of different mol% of MAAc on roughness, grain size, crystallinity, and bandgap of $MAPb_{0.75}Sn_{0.25}(I_{0.50}Br_{0.50})_3$ perovskite material.

4. Conclusion

We have successfully demonstrated the one step deposition process of pin hole free Sn-Pb based perovskite films spun from inks containing 50 mol% MAAc additive. Note that deposition of these inks by spin-casts does not require an anti-solvent step. The MAAc additive does not affect the bandgap and refractive index significantly. The films have full coverage with a roughness of around 13 nm and grain size around 64 nm. Film quality was confirmed by several characterization techniques. The films show a bandgap of around 1.63 eV and a 632.8 nm refractive index of 2.38. Our experiments confirm that these results are reproducible.

Acknowledgement

The authors acknowledge support of ONR (N00014-19-1-2576) and NSF (1927020).

References

[1] Z. Zhang *et al.*, "Balancing crystallization rate in a mixed Sn-Pb perovskite film for efficient and stable perovskite solar cells of more than 20% efficiency," *J. Mater. Chem. A*, vol. 9, no. 33, pp. 17830–17840, 2021, doi: 10.1039/d1ta04922d.

[2] S. Lv *et al.*, "Antisolvent-Free Fabrication of Efficient and Stable Sn–Pb Perovskite Solar Cells," *Sol. RRL*, vol. 5, no. 11, pp. 1–8, 2021, doi: 10.1002/solr.202100675.

[3] M. G. Ju *et al.*, "Toward Eco-friendly and Stable Perovskite Materials for Photovoltaics," *Joule*, vol. 2, no. 7, pp. 1231–1241, 2018, doi: 10.1016/j.joule.2018.04.026.

[4] Y. Li *et al.*, "50% Sn-Based Planar Perovskite Solar Cell with Power Conversion Efficiency up to 13.6%," *Adv. Energy Mater.*, vol. 6, no. 24, 2016, doi: 10.1002/aenm.201601353.

[5] F. Zuo, S. T. Williams, P. W. Liang, C. C. Chueh, C. Y. Liao, and A. K. Y. Jen, "Binary-Metal Perovskites Toward High-Performance Planar-Heterojunction Hybrid Solar Cells," *Adv. Mater.*, vol. 26, no. 37, pp. 6454–6460, 2014, doi: 10.1002/adma.201401641.

[6] Y. Ogomi *et al.*, "CH3NH3SnxPb(1-x)I3 perovskite solar cells covering up to 1060 nm," *J. Phys. Chem. Lett.*, vol. 5, no. 6, pp. 1004–1011, 2014, doi: 10.1021/jz5002117.

[7] Z. Yang *et al.*, "Stabilized Wide Bandgap Perovskite Solar Cells by Tin Substitution," *Nano Lett.*, vol. 16, no. 12, pp. 7739–7747, 2016, doi: 10.1021/acs.nanolett.6b03857.

[8] G. A. Tosado, Y. Y. Lin, E. Zheng, and Q. Yu, "Impact of cesium on the phase and device stability of triple cation Pb-Sn double halide perovskite films and solar cells," *J. Mater. Chem. A*, vol. 6, no. 36, pp. 17426–17436, 2018, doi: 10.1039/c8ta06391e.

[9] Z. Yang, A. Rajagopal, and A. K. Y. Jen, "Ideal Bandgap Organic–Inorganic Hybrid Perovskite Solar Cells," *Adv. Mater.*, vol. 29, no. 47, pp. 1–7, 2017, doi: 10.1002/adma.201704418.

[10] G. Kapil *et al.*, "Tin-Lead Perovskite Fabricated via Ethylenediamine Interlayer Guides to the Solar Cell Efficiency of 21.74%," *Adv. Energy Mater.*, vol. 11, no. 25, pp. 2–4, 2021, doi: 10.1002/aenm.202101069.

[11] J. Cao *et al.*, "High-Performance Tin–Lead Mixed-Perovskite Solar Cells with Vertical Compositional Gradient," *Adv. Mater.*, vol. 34, no. 6, pp. 1–10, 2022, doi: 10.1002/adma.202107729.

[12] Z. Zhu, N. Li, D. Zhao, L. Wang, and A. K. Y. Jen, "Improved Efficiency and Stability of Pb/Sn Binary Perovskite Solar Cells Fabricated by Galvanic Displacement Reaction," *Adv. Energy Mater.*, vol. 9, no. 7, pp. 1–22, 2019, doi: 10.1002/aenm.201802774.

[13] L. Ji *et al.*, "Band alignment of Pb-Sn mixed triple cation perovskites for inverted solar cells with negligible hysteresis," *J. Mater. Chem. A*, vol. 7, no. 15, pp. 9154–9162, 2019, doi: 10.1039/c8ta11891d.

[14] C. Li *et al.*, "Reducing Saturation-Current Density to Realize High-Efficiency Low-Bandgap Mixed Tin–Lead Halide Perovskite Solar Cells," *Adv. Energy Mater.*, vol. 9, no. 3, pp. 1–9, 2019, doi: 10.1002/aenm.201803135.

[15] Y. Xiao, L. Yang, G. Han, Y. Li, M. Li, and H. Li, "Effects of methylammonium acetate on the perovskite film quality for the perovskite solar cell," *Org. Electron.*, vol. 65, pp. 201–206, 2019, doi: 10.1016/j.orgel.2018.11.020.

[16] Y. Xia *et al.*, "Management of perovskite intermediates for highly efficient inverted planar heterojunction perovskite solar cells," *J. Mater. Chem. A*, vol. 5, no. 7, pp. 3193–3202, 2017, doi: 10.1039/c6ta09554b.

[17] S. Venkatesan *et al.*, "Moisture-driven phase transition for improved perovskite solar cells with reduced trap-state density," *Nano Res.*, vol. 10, no. 4, pp. 1413–1422, 2017, doi: 10.1007/s12274-017-1515-5.

[18] C. Q. Howlader, M. Hasan, A. Zakhidov, and M. Chen, "Optical dispersion study of PPDT2FBT by spectroscopic ellipsometry," vol. 1127712, no. February 2020, p. 38, 2020, doi: 10.1117/12.2545426.

[19] C. Howlader, M. Hasan, A. Zakhidov, and M. Y. Chen, "Determining the refractive index and the dielectric constant of PPDT2FBT thin film using spectroscopic ellipsometry," *Opt. Mater. (Amst).*, vol. 110, no. October, p. 110445, 2020, doi: 10.1016/j.optmat.2020.110445.